2024 IEEE International Conference on Robotics and Automation (ICRA 2024)
May 13-17, 2024. Yokohama, Japan

Robotic Manipulation of Hand Tools: The Case of Screwdriving

Ling Tang[1], Yan-Bin Jia[1], and Yuechuan Xue[2]

Abstract— **Despite decades of steady research progress, the robotic hand is still far behind the human hand in terms of dexterity and versatility. A milestone in this quest for human-level performance will be possessing the skills of manipulating hand tools, for their non-trivial geometries and for the intricacies of controlling their contact-based interactions with objects, which are the final targets of manipulation. This paper investigates screwdriving by a robotic arm/hand pair, dealing with the chain of contacts connecting the substrate, screw, screwdriver, and fingertips. Considering rolling contacts and finger gaits, our force control scheme is derived through backward chaining to leverage the dynamics of the screwdriver and arm/hand. To maintain the fastening effort, estimations are carried out sequentially for the screwdriver's pose via optimization under visual and kinematic constraints, and for its applied wrench on the screw via solution drawing upon dynamics. This wrench, adjusted based on position/force feedback, is mapped by the grasp matrix to the desired fingertip forces, which are then used for computing torques to be exerted by the arm and hand to close the loop. Simulation and experiments with a Shadow Hand have been conducted for validations.**

I. Introduction

Robots with human-level dexterity have long been a dream for the public and a goal for researchers. One of the most convincing proofs would be their ability to manipulate hand tools, which are designed for humans and have evolved for day-to-day jobs since ancient times. Aside from technical challenges that need to be overcome, possession of tool skills will enable robots to not only assist people in a wide range of activities — from household chores to medical operations and even to space missions — but also interact with them more closely and effectively.

As of today, robots often use specially designed and premounted tools, most of which are electrical (e.g., screwdriving systems [1], [2], [3]). A manual tool, if applied, usually needs to be modified in advance (e.g., handle enlargement for a wrench [4]). Further, the task environment often has to be engineered in a way that bears little resemblance to the home environment and impedes human-robot interactions. The main obstacle lies in the lack of robust algorithms to equip robots with for grasping and maneuvering tools in a natural setting. Until today, robotic hands cannot reliably pick up hand tools resting on a table, or any generally positioned objects with moderate shape complexities for that matter, not to mention eventually hold them in power grasps.

Robotic manipulation has been mostly concerned with altering the state of an object in direct contact with a robot. Hand tool manipulation bears the distinction that the manipulated tool is instead interacting with an object, which is the intended target of manipulation. Namely, the object is *indirectly* manipulated. This paper investigates manipulation of such a tool, more specifically, a screwdriver, to tighten a screw. In order to focus on the fastening operation, we make three assumptions below:

1) The robotic hand has already achieved a dexterous grasp on the screwdriver's handle.
2) The screw has been premounted into a threaded hole.
3) The screwdriver's tip is already engaged in contact with the bottom of the screw's drive.

The first assumption above relieves us from considering grasp achievement, a challenge by itself as mentioned earlier[3]. The second assumption is justified because premounting a screw by the robotic hand would require a level of finesse not reached today. As for the third assumption, the first two authors recently presented a procedure for mounting the screwdriver on the screw head via compliant sliding and rotation realized under impedance and hybrid position/admittance controls [6].

In our task, the screwdriver is manipulated by a robotic hand driven by a robotic arm. With its tip in the screw's drive under Assumption 2, the screwdriver may pivot about the tip's bottom edge. The arm, hand, screwdriver, and screw together form a kinematic chain with the last three connected through contacts. We approach the problem in a manner of backward chaining. First, the screwdriver keeps applying some torque on the screw in order to drive it into the tapped hole in the substrate. Just like screwdriving by the human hand, the reaction force/torque on the screwdriver's tip by the substrate via the screw needs to be "felt" as feedback, despite the absence of sensing at the tip contact. We can leverage the screwdriver dynamics to solve for this force. The solution requires knowledge about the screwdriver's pose, which is estimated using images taken by a camera and contact constraints imposed by the fingertips (whose poses are known from the hand kinematics) and the screwdriver's tip (which touches the bottom of the screw's drive). Force estimation also draws upon some primitive modeling of the screw-substrate interaction.

A desired resultant wrench by the hand is in need for multiple purposes: to control the fastening speed, to exert proper downward force, all in the axial direction, and to correct any small deviation of the screw before jamming happens. Such a wrench, derived via control, is then distributed over the fingertips as contact forces via inverting a grasp matrix that describes their placements on the handle. Changes in this

[1]Ling Tang and Yan-Bin Jia are with the Department of Computer Science, Iowa State University, Ames, IA 50011, USA. ling, jia@iastate.edu

[2]Yuechuan Xue is with Amazon, Cambridge, MA 02142, USA. yuechxue@amazon.com.

[3]Some recent effort [5] by the authors exploited the use of pivoting and finger gaiting.

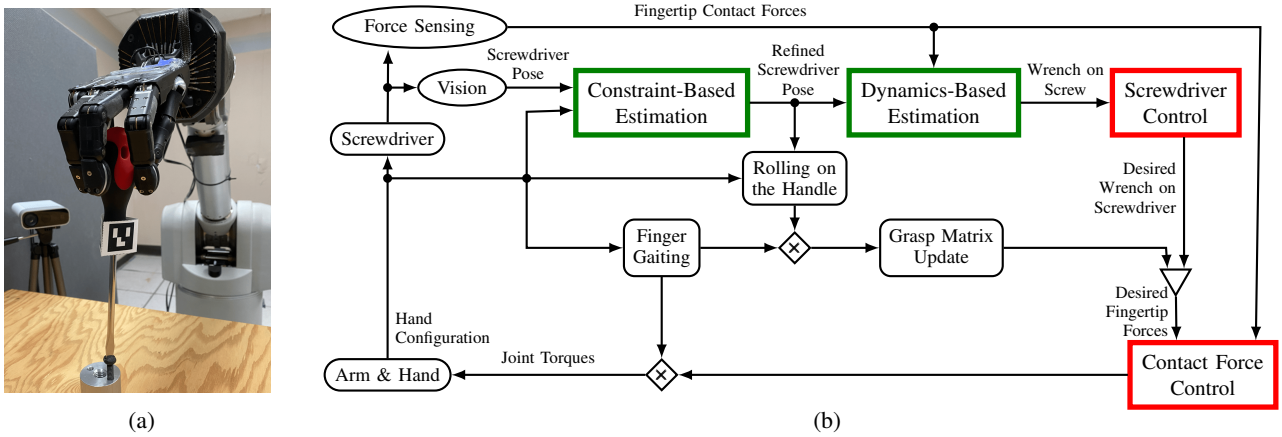

(a) (b)

Fig. 1: (a) Screwdriving by a Shadow Hand mounted on an WAM arm. (b) Architecture of the system of robotic screwdriving.

matrix are caused by rolling finger contacts on the handle, as well as by finger gaits performed from time to time for fastening to continue. To close the loop, the arm and hand are controlled based on their dynamics to realize desired finger contact forces, and finger gaits as investigated in [5].

Fig. 1(b) illustrates the architecture of the screwdriving system. There are two estimation modules, for the pose of the screwdriver and the torquing wrench on the screw, respectively, and two control modules, to generate the resultant wrench by the fingers on the screwdriver's handle and the torques to drive the arm and hand. Accompanying torque control are finger rolling kinematics and gaiting strategies. The estimation modules will be described in Section III and the control modules in Section IV.

II. Related Work

Robotic tool usage has been considered from the aspects of tool recognition based on extraction of visual and motor sensory data [7], [8], and of tool grasping and orienting approached via mechanics-based planning [9], [8], [10] or deep learning [11], [12], [13]. Demonstrations have been conducted on tasks such as light bulb screwing [14], bolt unscrewing [15], object twirling [16], drilling and pencil drawing [17], bottle opening and plant watering [18], etc. The level of exhibited dexterity, however, has been quite primitive, in large part due to ignorance of friction and compliance [19] and force control [20], [21], [22]. Hand tools requiring moderate skills have not been considered so far.

Threaded fastening [23] is basic for manufacturing and common in household maintenance. Past research investigated modeling [24], [25], [26], analysis [27], and control [28], [29], [30]. Two threaded parts could be aligned under visual guidance [31], [32] or based on force and position data [33]. Fastening efforts were eased using special-purpose end-effectors [34], [35], [36], or electric screwdrivers and wrenches [30], [37].

The kinematics of spatial motion with point contact was first studied in [38], and then separately derived as a system of differential equations with a specialization to rolling [39]. Forward kinematics of a multifingered hand and contact kinematics of rolling were combined to solve for the finger motions necessary to achieve a desired object motion [40]. In [41], a control law enabled a multifingered hand to make its grasped object track a given trajectory, by integrating kinematics of rolling, hand dynamics, as well as force closure under Coulomb friction. In [42], a robot leveraged rolling to first move its contacts into a "stable region", and then drive them to the desired locations. Other control algorithms based on rolling contact were developed for manipulation with two arms [43], four spherical fingertips [44], deformable fingertips [45], and of multiple objects [46].

The human hand applies finger gaits to adjust its grip, impart a particular motion of the grasped object, and operate a tool. The initial use of gaits by robotic fingers for "twirling" [47] was followed mostly by theoretical inquiries [48], [49], [50], [51], often under some strict assumptions. A finger gait was described as a discrete-continuous dynamic system [52], [53], [54], yielding gait control strategies [55], [56], [57] that were either simulated or experimentally demonstrated over simple shapes such as spheres, blocks, and cylinders. Gait sequences were planned by exploring various spaces of hybrid states [58], [59], for special underactuated hands [60], or under strict assumptions about simple shapes [61], [62].

III. Screwdriver Status Estimation

We place the world frame $\mathcal{F}_w$ at the base of the robotic arm. The screwdriver is a slotted one with a tool frame $\mathcal{F}$ attached at the center ${}^w\boldsymbol{p}$ of its tip's bottom edge (treated as a line segment)[4]. The frame's x-axis is along the edge and z-axis is aligned with the screwdriver's axis while pointing outward. See Fig. 2.

From our own screwdriving experience, the contact between the screwdriver's tip and the screw's drive acts most of the time like a hinge with one

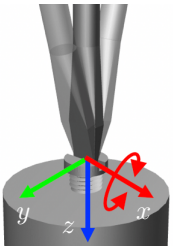

Fig. 2: Tool frame with 1-DOF about its x-axis to represent tilting.

[4]From now on, a term with the superscript ^{w} is expressed in the world frame $\mathcal{F}_w$ and one with no superscript is expressed in the tool frame $\mathcal{F}$.

DOF allowing the tip to tilt forward or backward. It is thus reasonable for us to assume that the tip has restricted y-axial rotation, and maintains the contacts with the two walls of the screw's drive. We propose contact-based estimation of the screwdriver's pose and dynamics-based estimation of the reaction force/torque from the screw on the screwdriver.

A. Screwdriver Pose From Finger Contacts

In a dexterous manipulation task, pose estimation solely relying on vision cannot provide the needed accuracy. Here we propose a method that takes an estimated tool pose from vision and polishes it under contact constraints imposed by fingertips.

The screwdriver's pose describes the tool frame $\mathcal{F}$, whose origin ${}^w\boldsymbol{p}$ is in contact with the screw's drive and close to its center ${}^w\boldsymbol{p}_s$. Note that we can estimate ${}^w\boldsymbol{p}_s$ quite well from the initial position of the screw and the amount of rotation by the screwdriver. Let $\boldsymbol{r}$ be the quaternion that describes the orientation of $\mathcal{F}$ relative to the world frame $\mathcal{F}_w$. The initial estimate $\bar{\boldsymbol{r}}$ of $\boldsymbol{r}$ is provided by vision. It is to be polished through constrained maximization.

Since the screwdriver's tip edge is in contact with the bottom of the screw's drive, we have the first constraint:

$$||{}^w\boldsymbol{p} - {}^w\boldsymbol{p}_s|| \leq \epsilon_1, \tag{1}$$

where ϵ_1 is some error tolerance. This constraint imposes that the tip does not "slide" in the drive.

The next are three sets of constraints which ensure that each finger contact "agrees with" the corresponding contact on the handle in both location and geometry. Before describing the constraints, we need to introduce some notations. For succinctness, the orientation of $\mathcal{F}$ in $\mathcal{F}_w$ is now denoted by a rotation matrix R. The handle's surface is described by a patch $\boldsymbol{\sigma}$ in the tool frame $\mathcal{F}$ such that $\boldsymbol{\sigma}(\xi_i, \eta_i)$, $1 \leq i \leq k$, locates its contact point with the i-th fingertip. Let the point ${}^w\boldsymbol{p}_i$ and matrix R_i be the location and rotation of the i-th fingertip's body frame $\mathcal{F}_i$ relative to $\mathcal{F}_w$. (Both can be calculated based on the forward kinematics of the arm and hand.) The fingertip has its surface described by a patch $\boldsymbol{\sigma}_i$ in $\mathcal{F}_i$ such that $\boldsymbol{\sigma}_i(u_i, v_i)$ locates the same contact point with the screwdriver's handle.

The fingertip contact constraints are, for $1 \leq i \leq k$,

$$||(R\boldsymbol{\sigma}(\xi_i, \eta_i) + {}^w\boldsymbol{p}) - (R_i\boldsymbol{\sigma}_i(u_i, v_i) + {}^w\boldsymbol{p}_i)|| \leq \epsilon_1, \tag{2}$$

$$|(R\hat{\boldsymbol{\sigma}}_\xi(\xi_i, \eta_i)) \cdot (R_i\hat{\boldsymbol{n}}_i(u_i, v_i))| \leq \epsilon_2, \tag{3}$$

$$|(R\hat{\boldsymbol{\sigma}}_\eta(\xi_i, \eta_i)) \cdot (R_i\hat{\boldsymbol{n}}_i(u_i, v_i))| \leq \epsilon_2, \tag{4}$$

where $\hat{\boldsymbol{\sigma}}_\xi$ and $\hat{\boldsymbol{\sigma}}_\eta$ are the unit vectors respectively along the partial derivatives of $\boldsymbol{\sigma}$ with respect to ξ and η, $\hat{\boldsymbol{n}}_i$ is the unit normal at the contact on the i-th finger, and ϵ_2 is the second error tolerance. For the i-th finger, the constraint (2) states that its contact point "coincides" with that on the handle, and the constraints (3) and (4) state that the tangent planes at the two points "coincide" with each other.

To respect the continuity of a rolling motion on the handle, we require that each finger contact $\boldsymbol{\sigma}(\xi_i, \eta_i)$ on the handle does not move significantly from its position $\boldsymbol{\sigma}(\xi_i^-, \eta_i^-)$ at the previous time instant. This induces an extra constraint:

$$(\xi_i - \xi_i^-)^2 + (\eta_i - \eta_i^-)^2 \leq \epsilon_3. \tag{5}$$

Finally, the pose optimization problem is formulated as

$$\max_{\substack{{}^w\boldsymbol{p}, \boldsymbol{r}, \\ u_1, v_1 \ldots, u_k, v_k \\ \xi_1, \eta_1, \ldots, \xi_k, \eta_k}} \quad |\boldsymbol{r} \cdot \bar{\boldsymbol{r}}| \tag{6}$$

subject to the constraints (1)–(5). In the objective function, the inner product is performed on the two quaternions $\boldsymbol{r}$ and $\bar{\boldsymbol{r}}$ as 4-vectors[5]. The optimization can be solved using the interior point optimizer (IPOPT) software [64]. This yields a pose of the screwdriver that not only is close to its initial estimate, but also satisfies all the kinematic constraints.

B. Wrench Passed Onto the Screwdriver From the Screw

To control the torquing wrench applied by the screwdriver to the screw, we need to estimate the force/toque transmitted from the substrate through the screw to the screwdriver tip.

Denote by $\boldsymbol{\nu} = (\boldsymbol{v}^\top, \boldsymbol{\omega}^\top)^\top$ the linear and angular velocities of the tool frame $\mathcal{F}$ as expressed in itself. The Newton-Euler equations governing the screwdriver dynamics are expressed in $\mathcal{F}$ as

$$\boldsymbol{F}_s + \boldsymbol{F}_h = M\dot{\boldsymbol{\nu}} + \boldsymbol{C} \tag{7}$$

where $\boldsymbol{F}_s = (\boldsymbol{f}_s^\top, \boldsymbol{\tau}_s^\top)^\top$ is the force/torque exerted by the screw, and $\boldsymbol{F}_h = (\boldsymbol{f}_h^\top, \boldsymbol{\tau}_h^\top)^\top$ is the resultant force/torque applied on the screwdriver by the robotic hand. Let $\boldsymbol{o}$ be the position of the screwdriver's center of mass in $\mathcal{F}$, and I be its inertial tensor expressed in a frame at $\boldsymbol{o}$ with the same orientation of $\mathcal{F}$. The mass matrix M in (7) has the form

$$M = \begin{bmatrix} mI_{3\times 3} & -m[\boldsymbol{o}]_\times \\ m[\boldsymbol{o}]_\times & I - m[\boldsymbol{o}]_\times[\boldsymbol{o}]_\times \end{bmatrix},$$

where the operator $[\cdot]_\times$ generates an 3×3 antisymmetric matrix that performs the cross product of the operand with any 3-vector through left multiplication. The term

$$\boldsymbol{C} = \begin{bmatrix} m([\boldsymbol{\omega}]_\times\boldsymbol{v} + [\boldsymbol{\omega}]_\times[\boldsymbol{\omega}]_\times\boldsymbol{o} - R^\top\boldsymbol{g}) \\ [\boldsymbol{\omega}]_\times(I - m[\boldsymbol{o}]_\times[\boldsymbol{o}]_\times)\boldsymbol{\omega} + m[\boldsymbol{o}]_\times([\boldsymbol{\omega}]_\times\boldsymbol{v} - R^\top\boldsymbol{g}) \end{bmatrix}$$

contains the fictitious force and gravity terms. We can estimate $\boldsymbol{\omega}$ by differentiating the pose of the screwdriver obtained through optimization in Section III-A. The matrices M and C can be evaluated. The resultant force/torque $\boldsymbol{F}_h$ exerted by the hand on the screwdriver is obtained by mapping the contact forces ${}^w\boldsymbol{f}_1, \ldots, {}^w\boldsymbol{f}_k$ exerted (and sensed) by the fingertips on the screwdriver's handle, using the grasp matrix G determined by the hand configuration. More specifically, $\boldsymbol{F}_h = \text{diag}[R^\top, R^\top]G({}^w\boldsymbol{f}_1^\top, \ldots, {}^w\boldsymbol{f}_k{}^\top)^\top$.

The system (7) of six equations is under-constrained because it has 6 unknowns in $\boldsymbol{F}_s$ and 6 more in $\dot{\boldsymbol{\nu}}$. Let the linear velocity $\boldsymbol{v}$ be $(v_x, v_y, v_z)^\top$, and the angular velocity $\boldsymbol{\omega}$ be $(\omega_x, \omega_y, \omega_z)^\top$. Since there is no sliding of the screwdriver's tip and the screw is fully constrained in the substrate, $\dot{v}_x = \dot{v}_y = 0$. It follows from the screw motion that $v_z = \frac{p}{2\pi}\omega_z$ and thus $\dot{v}_z = \frac{p}{2\pi}\dot{\omega}_z$, where p is the pitch of the screw. We

[5]It uses the metric Φ_4 for quaternions defined in [63].

also have $\dot{\omega}_y = 0$ since the screwdriver's rotation about its y-axis is prohibited by the drive's bottom as assumed earlier.

The torque $\boldsymbol{\tau}_s$ by the screw has three components $\tau_{s,x}$, $\tau_{s,y}$, and $\tau_{s,z}$ along the x-, y-, and z-axes of the tool frame $\mathcal{F}$. Since the screwdriver can rotate about its x-axis, the resistance torque about the axis is negligible, i.e., $\tau_{s,x} = 0$. The relationship between the fastening torque and the screw's turning angle has been investigated and modeled in the past [27], [65]. Excluding the initial mating and final over-tightening phases, we can model $\tau_{s,z}$ as a linear function $\tau_{s,z} = k_s\theta$, where k_s is some stiffness coefficient, and θ is the screw's total amount of axial rotation (estimated from the rotation of the screwdriver).

Hence, a total of six force and acceleration variables are known, which allows us to rewrite (7) as the following:

$$(\boldsymbol{f}_s^\top, 0, \tau_{s,y}, k_s\theta)^\top + \boldsymbol{F}_h = M\left(0, 0, \frac{p}{2\pi}\dot{\omega}_z, \dot{\omega}_x, 0, \dot{\omega}_z\right)^\top + \boldsymbol{C}.$$

Solving the above linear equation for $\boldsymbol{f}_s$, $\tau_{s,y}$, $\dot{\omega}_x$, and $\dot{\omega}_z$, we will use the obtained $\boldsymbol{F}_s = (\boldsymbol{f}_s^\top, 0, \tau_{s,y}, k_s\theta)^\top$ later for control of the screwdriver.

IV. Torquing by Arm/Hand

The screwdriver is engaged in two types of contacts, with the screw at its tip and the fingers on its handle. We employ hybrid position/force control on the hand summarized by the flow chart below:

$$\begin{array}{ccccccccc} {}^w\boldsymbol{x} & \xrightarrow{(9)} & \boldsymbol{\nu} & \xrightarrow{(10)} & \boldsymbol{\alpha} & & & \xrightarrow{(18)} & \\ & & & & \downarrow{\scriptstyle (8)} & & & & \\ \boldsymbol{F}_s & \xrightarrow{(11)} & \boldsymbol{F}_{sc} & \xrightarrow{(8)} & \boldsymbol{F}_{hd} & \xrightarrow{(15),\,(16)} & {}^w\boldsymbol{F}'_d & \xrightarrow{(18)} & \boldsymbol{\tau} \end{array}$$

The screwdriver's pose ${}^w\boldsymbol{x}$ (estimated in III-A) is differentiated to obtain the tool velocity $\boldsymbol{\nu}$. From them a position control servo $\boldsymbol{\alpha}$ is constructed. Using the wrench $\boldsymbol{F}_s$ (estimated in III-B) exerted by the screw, we derive a force servo $\boldsymbol{F}_{sc}$ to regulate the the force between the screw and the tool tip. From the two servos we can construct the desired resultant wrench $\boldsymbol{F}_{hd}$ by the hand on the tool via hybrid control. The wrench under the grasp matrix is mapped to the desired fingertip forces $\boldsymbol{F}'_d$. Finally, the arm/hand torque $\boldsymbol{\tau}$ is composed to realize the desired motion and wrench.

A. Desired Hand Wrench

Control of the screwdriver, conducted within the tool frame $\mathcal{F}$, aims at finding a desired wrench $\boldsymbol{F}_{hd}$ applied by the hand. We utilize the dynamics of the screwdriver (7) expressed in the tool frame $\mathcal{F}$ by replacing $\boldsymbol{F}_h$ with $\boldsymbol{F}_{hd}$, and $\boldsymbol{F}_s$ and $\dot{\boldsymbol{\nu}}$ respectively with control servos $\boldsymbol{F}_{sc}$ and $\boldsymbol{\alpha}$ (to be determined shortly). This yields

$$\boldsymbol{F}_{sc} + \boldsymbol{F}_{hd} = M\boldsymbol{\alpha} + \boldsymbol{C}. \tag{8}$$

While the "actual" dynamics of the screwdriver in (7) provides us an estimate of the force/torque exerted by the screw, the "desired" dynamics of the screwdriver is described by (8) and realized via error compensation.

Let $\boldsymbol{\gamma}$ be the z-y-x Euler angles[6] of the rotation of $\mathcal{F}$ from $\mathcal{F}_w$, and T be a matrix that transforms the Euler angle rates into the angular velocity in $\mathcal{F}_w$. The velocity and angular velocity of $\mathcal{F}$ can be expressed in itself as $\boldsymbol{\nu} = \Lambda^w\dot{\boldsymbol{x}}$, where ${}^w\boldsymbol{x} = ({}^w\boldsymbol{p}^\top, \boldsymbol{\gamma}^\top)^\top$ and $\Lambda = \mathrm{diag}(R^\top, R^\top T)$. Differentiating this equation, we get $\dot{\boldsymbol{\nu}} = \Lambda^w\ddot{\boldsymbol{x}} + \dot{\Lambda}^w\dot{\boldsymbol{x}}$ which, under $\dot{v}_x = \dot{v}_y = 0$ and the screw motion, becomes

$$\dot{\boldsymbol{\nu}} = UR^\top T\ddot{\boldsymbol{\gamma}} + \dot{\Lambda}^w\dot{\boldsymbol{x}}, \tag{9}$$

where

$$U = \begin{bmatrix} 0 & 0 & 0 & 1 & 0 & 0 \\ 0 & 0 & 0 & 0 & 1 & 0 \\ 0 & 0 & p/2\pi & 0 & 0 & 1 \end{bmatrix}^\top.$$

To constrain the motion of the screwdriver's tip, we apply position control in the rotational directions and force control in the translational directions. We let the desired angle of screwdriver rotation be $\boldsymbol{\gamma}_d = (0, 0, \omega_d(t)\Delta t + \theta_{z0})$, where $\omega_d(t)$ gives the desired fastening speed at time t, and θ_{z0} is the screw's initial amount of axial rotation. Denote by $\boldsymbol{\gamma}_e = \boldsymbol{\gamma}_d - \boldsymbol{\gamma}$ the amount of rotation error, with $\boldsymbol{\gamma}$ estimated as in III-A. From (9) we construct a Proportional-Integral-Differential (PID) position control servo

$$\boldsymbol{\alpha} = UR^\top T(\ddot{\boldsymbol{\gamma}}_d + k_v\dot{\boldsymbol{\gamma}}_e + k_p\boldsymbol{\gamma}_e + k_i\int \boldsymbol{\gamma}_e\,\mathrm{dt}) + \dot{\Lambda}^w\dot{\boldsymbol{x}}, \tag{10}$$

where the gains k_v, k_p, and k_i are properly selected.

Force control in the translational directions is realized by setting $\boldsymbol{F}_{sc}$ in (8) as

$$\boldsymbol{F}_{sc} = \begin{bmatrix} \boldsymbol{f}_d + k_f\int(\boldsymbol{f}_d - \boldsymbol{f}_s)\,\mathrm{dt} \\ \boldsymbol{\tau}_s \end{bmatrix}, \tag{11}$$

where $\boldsymbol{f}_d$ is some desired force of whose value is to be discussed shortly, and $\boldsymbol{F}_s = (\boldsymbol{f}_s^\top, \boldsymbol{\tau}_s^\top)^\top$ are estimated in III-B. Substituting (10) and (11) into (8), we obtain the desired resultant force/torque $\boldsymbol{F}_{hd}$ that the hand needs to apply to the screwdriver.

A few remarks to make here. First, the desired components of $\boldsymbol{f}_d$ along the tangential directions are set to 0 in order to prevent excessive forces from causing the tip to slide. Second, the desired force component along the z-axis is set by experience. Third, we regulate the fastening speed by applying position control over rotation about the z-axis. Last, the shared objective of the position controls about the x- and y-axes is to correct the tilting error of the screwdriver.

B. Forces by Rolling Fingertips

Point contacts exist between the fingers and the handle. As long as the force at each finger contact lies within its friction cone, the finger will generally roll on the handle, for which the kinematics has been studied in the past [38], [41].

Denote $\boldsymbol{c}_i$ as the contact position on the i-th fingertip expressed in its body frame $\mathcal{F}_i$, and $\boldsymbol{c}'_i$ as the point coinciding with $\boldsymbol{c}_i$ on the screwdriver, expressed in the tool frame $\mathcal{F}$. Since the finger rolls on the handle without slipping, the points $\boldsymbol{c}_i$ and $\boldsymbol{c}'_i$ must have the same velocity. Further, the unit normals $\hat{\boldsymbol{n}}_i$ and $\hat{\boldsymbol{n}}'_i$ at these two points on the respective

[6]Here, the Euler angles are used instead of the quaternion $\boldsymbol{q}$ or rotation matrix R to avoid redundancy.

surfaces $\boldsymbol{\sigma}_i$ and $\boldsymbol{\sigma}$ must be opposite to each other. These constraints are precisely formulated below, for $1 \leq i \leq k$,

$$ {}^w\boldsymbol{p} + R\boldsymbol{c}'_i = {}^w\boldsymbol{p}_i + R_i\boldsymbol{c}_i, \tag{12} $$

$$ {}^w\dot{\boldsymbol{p}} + R(\boldsymbol{\omega} \times \boldsymbol{c}'_i) = {}^w\dot{\boldsymbol{p}}_i + R_i(\boldsymbol{\omega}_i \times \boldsymbol{c}_i), \tag{13} $$

$$ R\hat{\boldsymbol{n}}_i = -R_i\hat{\boldsymbol{n}}_i, \tag{14} $$

where ${}^w\boldsymbol{p}$ and ${}^w\boldsymbol{p}_i$ were introduced earlier as the locations of the frames $\mathcal{F}$ and $\mathcal{F}_i$ in the world frame, and $\boldsymbol{\omega}_i$ is the angular velocity of $\mathcal{F}_i$ described in itself. Differentiating (12) with respect to time and subtracting (13) from the result, we get $R\dot{\boldsymbol{c}}'_i = R_i\dot{\boldsymbol{c}}_i$. With the same surface parameterizations used in III-A, we have $\boldsymbol{c}_i = \boldsymbol{\sigma}_i(u_i, v_i)$ and $\boldsymbol{c}'_i = \boldsymbol{\sigma}(\xi_i, \eta_i)$. This allows us to rewrite $R\dot{\boldsymbol{c}}' = R_i\dot{\boldsymbol{c}}_i$ using the partial derivatives of $\boldsymbol{c}_i$ and $\boldsymbol{c}'_i$ with respect to their surface parameters $\boldsymbol{u}_i = (u_i, v_i)^\top$ and $\boldsymbol{\xi}_i = (\xi_i, \eta_i)^\top$. Combine the rewritten equation with the one from differentiating (14) with respect to time:

$$ \begin{bmatrix} R\frac{\partial \boldsymbol{c}'_i}{\partial \boldsymbol{u}_i} & -R_i\frac{\partial \boldsymbol{c}_i}{\partial \boldsymbol{\xi}_i} \\ R\frac{\partial \hat{\boldsymbol{n}}_i}{\partial \boldsymbol{u}_i} & R_i\frac{\partial \hat{\boldsymbol{n}}_i}{\partial \boldsymbol{\xi}_i} \end{bmatrix} \begin{bmatrix} \dot{\boldsymbol{u}}_i \\ \dot{\boldsymbol{\xi}}_i \end{bmatrix} = \begin{bmatrix} 0 & 0 \\ [R\hat{\boldsymbol{n}}'_i]_\times R & [R_i\hat{\boldsymbol{n}}_i]_\times R_i \end{bmatrix} \begin{bmatrix} \boldsymbol{\omega} \\ \boldsymbol{\omega}_i \end{bmatrix}. $$

During rolling, the contact points on both surfaces are updated by integrating $\dot{\boldsymbol{u}}_i$ and $\dot{\boldsymbol{\xi}}_i$, which are solved from the above equation, for $1 \leq i \leq k$. These updated contacts, together with the estimated screwdriver pose, trigger an update of the grasp matrix G, through which we obtain the desired fingertip forces on the screwdriver as

$$ {}^w\boldsymbol{F}_d = G^\dagger \mathrm{diag}[R, R]\boldsymbol{F}_{hd}. \tag{15} $$

In the above, $G^\dagger$ is the pseudo-inverse of G, and ${}^w\boldsymbol{F}_d = ({}^w\boldsymbol{f}_{1d}^\top, \ldots, {}^w\boldsymbol{f}_{kd}^\top)^\top$ contains the desired contact forces in $\mathcal{F}_w$ for generating the resultant wrench $\boldsymbol{F}_{hd}$ on the tool.

C. Dynamics-Based Force Control

Control of the fingers aims at applying an appropriate force at each contact to realize ${}^w\boldsymbol{F}_d$ so rolling continues. The control is conducted in the world frame $\mathcal{F}_w$. In order to keep the contact force of each finger inside its friction cone, we need to add an internal force in the null space of the grasp matrix G. The desired contact forces are modified as

$$ {}^w\boldsymbol{F}'_d = {}^w\boldsymbol{F}_d + (I - G^\dagger G){}^w\boldsymbol{F}_0, \tag{16} $$

where in the second summand, a vector ${}^w\boldsymbol{F}_0$ is projected to the null space of the grasp matrix. Addition of this term, with a proper choice of ${}^w\boldsymbol{F}_0$, can bring the contact forces inside their friction cones without changing the resultant force/torque on the screwdriver.

The velocities of all the contact frames are stacked as one vector and described in the world frame as ${}^w\boldsymbol{V} = G^\top R\boldsymbol{\nu}$. Let $\boldsymbol{q}$ be the vector consisting of the n joint angles of the arm-hand robot. For the i-th finger in contact, we have $\boldsymbol{v}_i = J_i\dot{\boldsymbol{q}}$, where J_i is the $3\times n$ linear Jacobian matrix at the contact. Stacking such equations of all contacts, we have ${}^w\boldsymbol{V} = J\dot{\boldsymbol{q}}$ where $J = (J_1^\top, \ldots, J_k^\top)^\top$. Hence, $J\dot{\boldsymbol{q}} = G^\top R\boldsymbol{\nu}$. Differentiating this equation with respect to time, we obtain the joint acceleration as

$$ \ddot{\boldsymbol{q}} = J^\dagger G^\top R\dot{\boldsymbol{\nu}} + J^\dagger G^\top \dot{R}\boldsymbol{\nu} + J^\dagger \dot{G}^\top R\boldsymbol{\nu} - J^\dagger \dot{J}\dot{\boldsymbol{q}}. \tag{17} $$

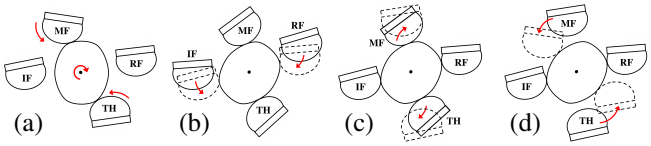

Fig. 3: Top view of the finger gaits to reset the hand configuration for recurrent screwdriving: (a) rolling of the thumb (TH) and the middle finger (MF) on the screwdriver for torquing; (b) addition of the index finger (IF) and the ring finger (RF) onto the screwdriver; (c) detaching of the TH and MF; (d) relocation of the TH and MF.

We have the dynamics of the robot in the world frame as

$$ \boldsymbol{\tau} = M_r\ddot{\boldsymbol{q}} + C_r\dot{\boldsymbol{q}} + \boldsymbol{N} + J^\top {}^w\boldsymbol{F}, \tag{18} $$

where M_r is the mass matrix, C_r contains the Coriolis and centrifugal term, $\boldsymbol{N}$ is the gravity term, and ${}^w\boldsymbol{F}$ is the stacked contact forces ${}^w\boldsymbol{f}_1, \ldots, {}^w\boldsymbol{f}_k$ exerted and also sensed by the fingertips on the screwdriver's handle. We obtain a hybrid controller in the following two steps:

- To realize position control of the screwdriver, we replace $\dot{\boldsymbol{\nu}}$ in (17) with the servo $\boldsymbol{\alpha}$ in (10) that regulates the pose of the tool, and plug the resultant $\ddot{\boldsymbol{q}}$ into (18).
- To realize force control, we replace ${}^w\boldsymbol{F}$ in (18) with ${}^w\boldsymbol{F}'_d + k_f\int {}^w\boldsymbol{F}_e\,\mathrm{d}t$, where ${}^w\boldsymbol{F}'_d$ is given in (16), and ${}^w\boldsymbol{F}_e = {}^w\boldsymbol{F}'_d - {}^w\boldsymbol{F}_S$ is the force errors between ${}^w\boldsymbol{F}'_d$ and the fingertip force readings ${}^w\boldsymbol{F}_S$.

The movements of the fingertips follow the contact positions on the handle under (17). Since we have no constraint over the orientation of a contact frame, each fingertip rotates to produce a rolling motion on the handle. The locations of the finger contacts need to be updated at each time instance via rolling kinematics.

D. Finger Gaiting

We let the thumb (TH) and middle finger (MF) perform the fastening task. Whenever a finger joint reaches its limit or the contact on a fingertip reaches the boundary of its tip surface, both TH and MF are relocated properly for the next round of screwdriving via finger gaits (see Fig. 3). Before either of them breaks contact, the index finger (IF) and ring finger (RF) are added on the screwdriver's handle to keep it in balance. Fig. 3(b) illustrates the additions of the IF and RF. An inverse kinematics problem is solved under the constraints that FF and MF are in contact with the handle, while the contact positions and normals on the hold fingers TH and MF do not change. The constraints for other relocating operations are established similarly.

To perform finger gaits, we use the same hybrid position/impedance control from our previous work [5] with some modifications. When the TH and MF are relocating themselves, the IF and RF are allowed to roll on the handle, which saves some DOFs needed by the operation.

V. Simulation and Experiment

We validate our approach via simulation and experiments with a Shadow Dexterous Hand mounted on the elbow of a Barrett 4-DOF WAM Arm.

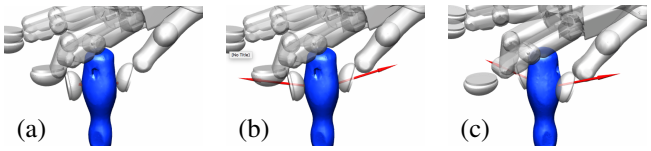

Fig. 4: (a) The screwdriver is held by the thumb and the middle finger initially. (b) The two fingers increase contact forces (represented by arrows to indicate directions as well as magnitudes). (c) The screwdriver is rotated.

A. Dynamics-Based Simulation

The simulation is conducted on the platform MuJoCo with the screwdriver designated as a free object. MuJoCo cannot simulate the complex interactions between the screw and the substrate. We get around this limitation by allowing the screw to rotate about its axis, while fixing the other five DOFs. A stiffness is assigned so the resistance torque increases as the screw rotates, which requires the fastening torque to increase as in a real screwdriving scenario. The pose of the screwdriver is read from the the simulator, with some random noise added to mimic realistic visual feedback. Then it is refined using the optimization in III-A. The force at each fingertip is also read from the the simulator to model force sensing. Fig. 4 illustrates a successful fastening maneuvered by the thumb and middle finger.

B. Experiment

The setup is shown in Fig. 1(a). To obtain an initial pose estimate of the screwdriver, we put ArUco markers [66] on its handle as shown in Fig. 5(a). An image frame was captured by an Azure Kinect camera, and processed using the OpenCV library to estimate the marker's pose in the camera's coordinate system. The result was then transformed into the screwdriver's pose in $\mathcal{F}_w$. The data from one time instant during a trial were visualized using MuJoCo in Fig. 5(b). The initial pose estimate (red) from vision deviated from the real one shown in (a) but was improved to an estimate (blue) via the pose optimization (6). Since the Shadow Hand was not equipped with tactile sensors, we employed a procedure from our previous work [5] to estimate the contact forces. A calibration function was used to map the hand's strain gauge readings to the joint torques, which were fed to forward dynamics for estimating the contact forces on fingertips[7].

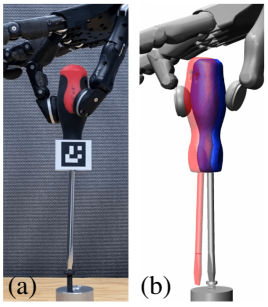

Fig. 5: (a) Experiment image. (b) Initial (red) and refined (blue) pose estimates of the screwdriver in (a).

The programming interface of the Shadow Hand accepts position commands only. Accordingly, we adapted our dynamics-based controller to generate equivalent position commands in four steps. First, we obtained the desired fingertip contact positions ${}^w\boldsymbol{X}_d$ by integrating $\boldsymbol{\alpha}$ in (10) twice, and mapping the result to the contact positions in the world frame. Note that ${}^w\boldsymbol{X}_d$ follows the screwdriver's error-compensated motion without applying force. Second, we computed the desired contact forces ${}^w\boldsymbol{F}'_d$ using (16). Third, we obtained the desired contact positions as ${}^w\boldsymbol{X}_c = {}^w\boldsymbol{X}_d + k_m {}^w\boldsymbol{F}'_d$ with k_m being some compliance, which allows their desired positions to penetrate into the handle's surface along the directions of ${}^w\boldsymbol{F}'_d$. Finally, ${}^w\boldsymbol{X}_c$ was mapped to the joint space by an iterative inverse Jacobian solver.

[7]The estimation deviated $\leq 25\%$ in magnitude and $\leq 30^\circ$ in direction.

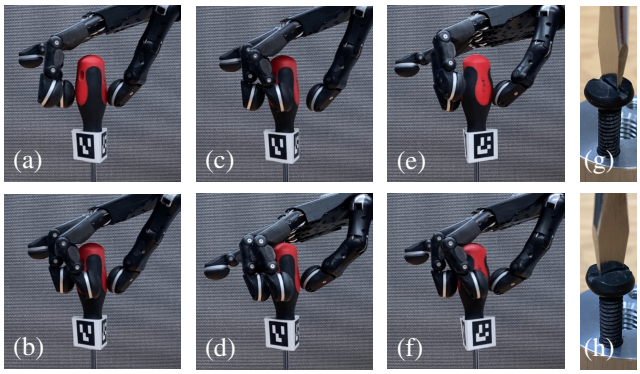

Fig. 6: The screwdriver handle is grasped by the TH and MF in (a), and then the IF and RF are added in (b). The first pair is removed in (c) and then relocated in (d). The second pair is then removed and, after the first pair has performed some screwdriving in (e), added back in (f) for the next round. (g) Before and (h) after three rounds of finger rolling and gaiting.

Fig. 6 shows a sequence of maneuvers, which took about 20 seconds. Twenty trials were conducted with seventeen exceeding five rounds of finger rolling and gaiting. Actions broke when the screwdriver's handle slipped off the fingers or its tip slid out of the screw's drive. The causes were often errors in contact updates during finger gaits. Other factors, such as errors in contact force estimates and vibrations of the Shadow Hand, could have also played a part.

VI. Discussion and Future Work

The described approach to the complex action of screwdriving by hand integrates estimation, contact modeling, rolling, finger gaiting, grasping, dynamics (of both the tool and robot), and controls (position and force). It can be adapted to other types of screwdrivers (e.g., a Phillips screwdriver) with different handle shapes.

Immediate next steps include stability analysis for the control strategies, improved estimation of the tool-fastener interaction force, robustness of real performance, and failure recovery. Later we will look at generalizing the approach to manipulation of other hand tools such as wrenches, pliers, and hammers. The next stage will be to further the study of tool grasping in natural settings and to integrate the findings with skills of tool maneuvering from the undergoing research, such that the robotic hand will have the ability to operate and switch between multiple tools for accomplishing a series of tasks.

Acknowledgment

We would like to thank Amazon Robotics AI for its donation of the Shadow Dexterous Hand used in this research, and the anonymous reviewers for their valuable comments.

REFERENCES

[1] https://www.youtube.com/watch?v=ThWwuId0Fas.

[2] https://www.youtube.com/watch?v=BOY3oZ8SkZU.

[3] https://www.youtube.com/watch?v=97mO2oa6Nsk.

[4] DARPA Robotics Challenge. https://www.darpa.mil/program/darpa-robotics-challenge.

[5] Y. Xue, L. Tang, and Y.-B. Jia. Dynamic finger gaits via pivoting and adapting contact forces. In *Proc. IEEE/RSJ Int. Conf. Intell. Robots Syst.*, pp. 8784–8791, 2023.

[6] L. Tang and Y.-B. Jia. Robotic fastening with a manual screw driver. In *Proc. IEEE Int. Conf. Robot. Autom.*, May 2023, pp. 5269–5275.

[7] I. Kresse, U. Klank, and M. Beetz. Multimodal autonomous tool analyses and appropriate application. In *Humanoids*, 2011, pp. 698–613.

[8] V. Tikhanoff, U. Pattacini, L. Natale, and G. Metta. Exploring affordances and tool use on the iCub. In *Humanoids*, 2013, pp. 130–137.

[9] S. Gupta, C. J. Paredis, and P. Brown. Micro planning for mechanical assembly operations. In *Proc. IEEE Int. Conf. Robot. Autom.*, 1998, pp. 239–246.

[10] M. Toussaint, K. Allen, K. A. Smith, and J. B. Tenenbaum. Differentiable physics and stable modes for tool-use and manipulation planning. In *Robotics: Sci. Syst.*, 2018.

[11] W. Li and M. Fritz. Teaching robots the use of human tools from demonstration with non-dexterous end-effectors. In *Humanoids*, 2015, pp. 547–553.

[12] N. Saito, K. Kim, S. Murata, T. Ogata, and S. Sugano. Detecting features of tools, objects, and actions from effects in a robot using deep learning. In *Proc. IEEE Int. Conf. Develop. Learning Epigenetic Robot.*, 2018, pp. 1–6.

[13] K. Fang, Y. Zhu, A. Garg, A. Kurenkov, V. Mehta, Li Fei-Fei, and S. Savarese. Learning task-oriented grasping for tool manipulation from simulated self-supervision. *Int. J. Robot. Res.*, vol. 39, no. 2–3, pp. 202–216, 2020.

[14] Y. Lin and Y. Sun. Grasp planning to maximize task coverage. *Int. J. Robot. Res.*, vol. 34, no. 9, pp. 1195–1210, 2015.

[15] T. Hasegawa, T. Suehiro, and K. Takase. A model-based manipulation system with skill-based execution. *IEEE Trans. Robot. Automat.*, vol. 8, no. 5, pp. 535–544, 1992.

[16] V. Kumar, E. Todorov, and S. Levine. Optimal control with learned local models: Application to dexterous manipulation. In *Proc. IEEE Int. Conf. Robot. Autom.*, 2016, pp. 378–383.

[17] H. Hoffmann, Z. Chen, D. Earl, D. Mitchell, B. Salemi, and J. Sinaopv. Adaptive robotic tool use under variable grasps. *Robot. Autonomous Sys.*, vol. 62, pp. 833–846, 2014.

[18] J. Stückler and S. Behnke. Adaptive tool-use strategies for anthropomorphic service robots. In *Humanoids*, 2014, pp. 755–760.

[19] M. T. Mason. Compliance and force control for computer controlled manipulators. *IEEE Trans. Syst., Man, Cybern.*, vol. SMC-11, no. 6, pp. 418–432, 1981.

[20] M. Raibert and J. Craig. Hybrid position/force control of manipulators. *ASME J. Dyn. Syst., Meas., Control*, vol. 103, no. 2, pp. 126–133, 1981.

[21] N. Hogan. Impedance control: An approach to manipulation: Parts I — III. *ASME. J. Dyn. Syst., Meas., Control*, vol. 107, pp. 1–24, 1985.

[22] O. Khatib. A unified approach for motion and force control of robot manipulators: The operational space formulation. *IEEE J. Robot. Automat.*, vol. 3, pp. 43–53, 1987.

[23] Z. Jia, A. Bhatia, R. M. Aronson, D. Bourne, and M. T. Mason. A survey of automated threaded fastening. *IEEE Trans. Autom. Sci. Eng.*, vol. 16, no. 1, pp. 298–310, 2019.

[24] E. J. Nicolson and R. S. Fearing. Dynamic modeling of a part mating problem: Thtreaded fasterner insertion. In *Proc. IEEE/RSJ Int. Conf. Intell. Robots Syst.*, 1991, pp. 30–37.

[25] S. Wiedmann and B. Sturges. Spatial kinematic analysis of threaded fastener assembly. *ASME J. Mech. Design*, vol. 128, pp. 116-127, 2006.

[26] S. Wiedmann and B. Sturges. A full kinematic model of thread-starting for assembly authomation analysis. *ASME J. Mech. Design*, vol. 128, pp. 128-136, 2006.

[27] L. Seneviratne, F. Ngemoh, and S. Earles. Theoretical modeling of screw tightening operations. In *Proc. ASME Eur. Joint Conf. Syst., Design Anal.*, 1992, pp. 189–192.

[28] T. Tsujimura and T. Yabuta. Adaptive force control of screwdriving with a positioning-controlled manipulator. *Robot. Auton. Syst.*, vol. 7, pp. 57–65, 1991.

[29] N. Dhayagude, Z. Gao, and F. Mrad. Fuzzy logic control of automated screw fastening. *Robot. Comput.-Integr. Manuf.*, vol. 12, no. 3, pp. 235–242, 1996.

[30] K. Pfeiffer, A. Escande, and A. Kheddar. Nut fastening with a humanoid robot. In *Proc. IEEE/RSJ Int. Conf. Intell. Robots Syst.*, 2017, pp. 6141–6148.

[31] B. Lara, K. Althoefer, and L. D. Seneviratne. Automated robot-based screw insertion system. In *Proc. 24th Annu. Conf. IEEE Ind. Electron. Soc.*, 1998, pp. 2440–2445.

[32] S. Pitipong, P. Pornjit, and P. Watcharin. An automated four-DOF robot screw fastening using visual servo. In *Proc. of IEEE/SICE Int. Symp. Syst. Integr.*, 2010, pp. 379–383.

[33] M. A. Diftler and Ian D. Walker. Experiments in aligning threaded parts using a robot hand. *IEEE Trans. Robot. Automat.*, vol. 15, no. 5, pp. 858–868, 1999.

[34] A. Cherubini, R. Passama, P. Fraisse, and A. Crosnier. A unified multimodal control framework for human robot interaction. *Robot. Auton. Syst.*, vol. 70, pp. 106–115, 2015.

[35] T. Matsuno, J. Huang, and T. Fukuda. Fault detection algorithm for external thread fastening by robotic manipulator using linear support vector machine classifier. In *Proc. IEEE Int. Conf. Robot. Autom.*, 2013, pp. 3443–3450.

[36] Y. Yokokohji, Y. Kawai, M. Shibata, Y. Aiyama, S. Kotosaka, W. Uemura, A. Noda, H. Dobashi, T. Sakaguchi, and K. Yokoi. Assembly challenge: A robot competition of the industrial robotics category, world robot summit–summary of the pre-competition in 2018. *Adv. Robot.*, vol. 33, no. 17, pp. 876–899, 2019.

[37] F. von Drigalski, et al. Team O2AS at the world robot summit 2018: An approach to robotic kitting and assembly tasks using general purpose grippers and tools. *Adv. Robot.*, vol. 34, no. 7-8, pp. 477–498, 2020.

[38] C. Cai and B. Roth. On the spatial motion of a rigid body with point contact. In *Proc. IEEE Int. Conf. Robot. Autom.*, 1987, pp. 686–695.

[39] D. J. Montana. The kinematics of contact and grasp. *Int. J. Robot. Res.*, vol. 7, no. 3, pp. 17–32, 1988.

[40] J. Kerr and B. Roth. Analysis of multifingered hands. *Int. J. Robot. Res.*, vol. 4, no. 4, pp. 3–17, 1986.

[41] A. A. Cole, P. Hsu, and S. Sastry. Kinematics and control of multifingered hands with rolling contact. *IEEE Trans. Autom. Control*, vol. 34, no. 4, pp. 398–404, 1989.

[42] K. Harada, T. Kawashima, and M. Kaneko. Rolling based manipulation under neighborhood equilibrium. *Int. J. Robot. Res.*, vol. 21, no. 5–6, pp. 463–474, 2002.

[43] N. Sarkar, X. Yun, and V. Kumar. Dynamic control of a 3-D rolling contacts in two-arm manipulation. *IEEE Trans. Robot. Automat.*, vol. 13, no. 3, pp. 364–376, November 1997.

[44] M. Cherif and K. K. Gupta. Global planning for dexterous reorientation of rigid objects: Finger tracking with rolling and sliding. *Int. J. Robot. Res.*, vol. 20, no. 1, pp. 57–84, 2001.

[45] Z. Doulgeri and J. Fasoulas. Grasping control of rolling manipulations with deformable fingertips. *IEEE/ASME Trans. Mechatron.*, vol. 8, no. 2, pp. 283–286, 2003.

[46] K. Harada, M. Kaneko, and T. Tsuji. Rolling-based manipulation for multiple objects. *Proc. IEEE Int. Conf. Robot. Autom.*, vol. 16, no. 5, pp. 457–468, 2000.

[47] R. S. Fearing. Implementing a force strategy for object re-orientation. In *Proc. IEEE Int. Conf. Robot. Autom.*, 1986, pp. 96–102.

[48] J. Hong, G. Lafferriere, B. Mishra, and X. Tan. Fine manipulation with multifinger hands. In *Proc. IEEE Int. Conf. Robot. Autom.*, 1990, pp. 1568–1573.

[49] L. Han and J. C. Trinkle. Dextrous manipulation by rolling and finger gaiting. In *Proc. IEEE Int. Conf. Robot. Autom.*, 1998, pp. 730–735.

[50] B. Goodwine and J. W. Burdick. Motion planning for kinematic stratified systems with application to quasi-static legged locomotion and finger gaiting. *IEEE Trans. Robot. Automat.*, vol. 18, no. 2, pp. 209–222, 2002.

[51] J. Xu and Z. Li. A kinematic model of finger gaits by multifingered hand as hybrid automaton. *IEEE Trans. Autom. Sci. Eng.*, vol. 5, no. 3, pp. 467–479, 2008.

[52] R. W. Brockett. Formal languages for motion description and map making. In R. W.Brockett et al., ed., *Robotics*, vol. 41, pp. 181–193. American Mathematical Society, Providence, RI, 1990.

[53] T. Henzinger. The theory of hybrid automata. In *Proc. 11th Annu. IEEE Symp. Logic Comput. Sci.*, 1996, pp. 278–292.
[54] M. S. Branicky, V. S. Borkar, and S. K. Mitter. A unified framework for hybrid control: model and optimal control theory. *IEEE Trans. Autom. Control*, vol. 43, no. 1, pp. 31–45, 1998.
[55] M. Buss and G. Schimit. Hybrid system behavior specification for multiple robotic mechanisms. In *Proc. IEEE/RSJ Int. Conf. Intell. Robots Syst.*, 1996, pp. 140–147.
[56] M. Huber and R. A. Grupen. Robust finger gaits from closed-loop controllers. In *Proc. IEEE/RSJ Int. Conf. Intell. Robots Syst.*, 2002, pp. 1578–1584.
[57] M. Pfanne, M. Chalon, F. Stulp, and H. Ritterand A. Albu-Schäffer. Object-level impedance control for dexterous in-hand manipulation. *IEEE Robot. Autom. Letters*, vol. 5, no. 2, pp. 2987–2994, 2020.
[58] J. Xu, T. K. J. Koo, and Z. Li. Sampling-based finger gaits planning for multifingered robotic hand. *Autonomous Robots*, vol. 28, pp. 385–402, 2010.
[59] K. Hang, M. Li, J. A. Stork, Y. Bekiroglu, F. T. Pokorny, A. Billard, and D. Kragic. Hierarchical fingertip space: A unified framework for grasp planning and in-hand grasp adaption. *IEEE Trans. Robot.*, vol. 32, no. 4, pp. 960–972, 2016.
[60] R. R. Ma and A. M. Dollar. An underactuated hand for efficient finger-gaiting-based dexterous manipulation. In *Proc. IEEE Int. Conf. Robot. Biomim.*, 2014, pp. 2214–2219.
[61] B. Sundaralingam and T. Hermans. Geometric in-hand regrasp planning: Alternating optimization of finger gaits and in-grasp manipulation. In *Proc. IEEE Int. Conf. Robot. Autom.*, 2018, pp. 231–238.
[62] A. S. Morgan, K. Hang, B. Wen, K. Bekris, and A. M. Dollar. Complex in-hand manipulation via compliance-enabled finger gaiting and multimodel planning. *IEEE Robot. Autom. Letters*, vol. 7, no. 2, pp. 4821–4828, 2022.
[63] D. Q. Huynh, Metric for 3D rotations: Comparisons and analysis. *J. Math. Imaging Vis.*, vol. 35, pp. 155–164, 2009.
[64] A. Wächter and L. T. Biegler. On the implementation of an interior-point filter line-search algorithm for large-scale nonlinear programming. *Math. Program.*, vol. 106, no. 1, pp. 25–57, 2006.
[65] J. Bickford. *Introduction to the Design and Behavior of Bolted Joints*. Boca Raton, FL, USA: CRC Press, 2007.
[66] S. Garrido-Jurado, R. Muñoz-Salinas, and F. J. Marín-Jiménez. Automatic generation and detection of highly reliable fiducial markers under occlusion. *J. Pattern Recog.*, vol. 47, no. 6, pp. 2280–2292, 2014.